

Selection of thinner for epoxy–amine system used as binder for polymeric mortars

Amal Bourguiba,^{1,2} Wadia Dhaoui,² Elhem Ghorbel¹

¹Laboratoire de Mécanique et Matériaux du Génie Civil (L2MGC), Université de Cergy Pontoise, 5, Mail Gay Lussac, Neuville-sur-Oise, 95000, Cergy, France

²Unité de Recherche de Chimie Minérale Appliquée (UR11ES18), Faculté des Sciences de Tunis, Université de Tunis El Manar, 2092, Campus Universitaire, Tunis, Tunisia

Correspondence to: E. Ghorbel (E-mail: elhem.ghorbel@u-cergy.fr)

ABSTRACT: Epoxy resin mortars are mainly used in the implementation of precast items used in the civil engineering field. The workability of these mortars represents a major obstacle to the development of this field. In order to improve this property, different types of thinners are selected to study their effect on the rheological properties of the epoxy–amine system. Rheological tests are performed in order to estimate the resin gel point and to measure its viscosity during the crosslinking reaction. It appears that viscosity is the lowest for mixtures prepared with methyl octanoate, *o*-xylene, and butyl glycidyl ether. Methyl octanoate is chosen as an ecofriendly thinner. The curing process is evaluated by varying the amount of the selected thinner using isothermal and dynamic DSC to determine the end of crosslinking. The mechanical properties using dynamic mechanical analysis (DMA) and tensile resistance testing of the cured epoxy resin with different amounts of methyl octanoate are also investigated. © 2016 Wiley Periodicals, Inc. *J. Appl. Polym. Sci.* 2016, 133, 43970.

KEYWORDS: crosslinking; kinetics; properties and characterization; structure–property relations; thermosets

Received 6 November 2015; accepted 22 May 2016

DOI: 10.1002/app.43970

INTRODUCTION

Epoxy resins are the most commonly used thermosets in polymer matrix composites.^{1–3} They have good adhesion to other materials and excellent chemical and environmental resistance. Owing to these outstanding characteristics, epoxy resins are widely used in various engineering and structural applications, such as in the electrical and aircraft industries.^{4–10} In the construction field, epoxy resins are used to replace the cement matrix in order to improve the resistance of mortars to environmental exposure. The resulting product is called “resin mortar.”^{11–13} Chemical and corrosion resistance, low permeability, and high thermal stability are some of the advantages that make these polymer composites suitable for precast components, the repair of engineering structures, and the implementation of mortars for industrial floors.^{14–19}

Several studies have focused on developing epoxy mortars to optimize their formulation and to investigate their mechanical properties and thermal stability.^{20–29} Although epoxy mortars exhibit high mechanical resistance and excellent durability, their low workability limits their development, even in the precast building field. This low workability is due to the high viscosity of the polymeric binder (epoxy–amine system). Therefore, to

achieve the desired properties, epoxy resin is used with additives like reactive and nonreactive thinners.^{30–33} Reactive thinners are molecules containing one or more than two epoxy groups. Their addition has the effect of lowering the viscosity of the resin while participating in the crosslinking reaction. Nonreactive thinners do not participate in the curing process but are physically mixed and dispersed. They include organic solvents (such as ketones and xylenes) and are typically used at less than 10 wt % of the prepolymer and hardener blend, in order to not affect the quality of the final product.³⁰

Hence, the main objective of this work is to find a thinner that can reduce the viscosity of the epoxy–amine system and consequently improve the mortar workability without altering the mechanical properties.

This paper deals with the effect of different types of thinners on the rheological and mechanical properties of an epoxy–amine system used as a binder in civil engineering applications. The aim is to select the optimal thinner in regards to the gel point, which must remain constant, to the viscosity, which has to be lowered, and to the optimal amount of the chosen thinner with reference to the mechanical and physical properties of the cured resin.

EXPERIMENTAL

Materials

The epoxy–amine system used was Eponal 371 provided by Bostik (Venette-France). The blend consists of a DGEBA-type epoxy resin (diglycidyl ether of bisphenol A) and a hardener based on an aliphatic amine. As this resin is used for a civil engineering applications, the two components contain silica and calcite fillers. The selected thinners (Table I) were methyl octanoate, *o*-xylene, butyl glycidyl ether, benzyl alcohol, and epoxidized soybean oil. They were all of analytical purity purchased from commercial sources (Sigma-Aldrich in Saint-Quentin Fallavier-France) and used directly without further purification.

Preparation of Samples

Rheological measurements of the epoxy–amine system were performed on mixtures prepared as follows. The resin and hardener were introduced into a beaker and were mixed under mechanical stirring for 3 min at a ratio of 100:60 by weight (resin/hardener) in accordance with the manufacturer recommendations. The chosen thinner (Table I) was added at 5 wt %.

The curing process and mechanical properties of the epoxy–amine system were investigated on mixtures prepared as described above by varying the amount of methyl octanoate (an ecofriendly thinner selected for its ability to reduce viscosity). The sample amounts of methyl octanoate were 2 wt %, 5 wt %, 7 wt %, and 9 wt %.

Rheological Measurements

A plate–plate rheometer, the Haake RheoWin RT 20 with a diameter of 20 mm (Karlsruhe, Germany), was used to estimate the gel point of the epoxy–amine system and to measure its vis-

cosity. The tests were conducted in isothermal mode at 30 °C under a constant strain ($\gamma_0 = 2\%$) and fixed angular frequency, $\omega = 10 \text{ rad s}^{-1}$. The applied strain γ^* and the resulting shear stress τ^* are described by eqs. 1 and 2. The test allowed us to calculate the complex shear modulus G^* [eq. 3] and the dynamic complex viscosity η^* [eq. 4]

$$\gamma^*(\omega) = \gamma_0 e^{i\omega t} \quad (1)$$

$$\tau^*(\omega) = \tau_0 e^{i(\omega t + \delta)} \quad (2)$$

$$G^* = G' + iG'' \quad (3)$$

$$\eta^*(\omega) = \frac{G^*(\omega)}{i\omega} \quad (4)$$

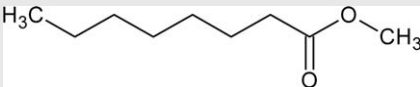
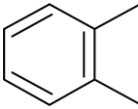
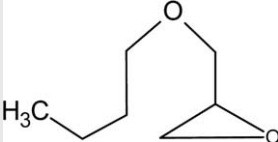
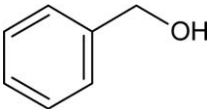
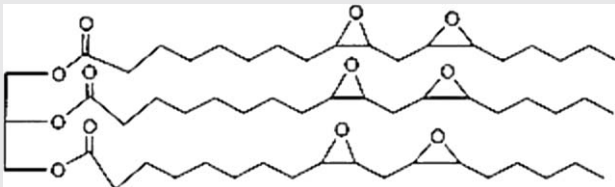
where δ is the phase shift between the applied strain γ^* and the resulting shear stress τ^* , and i is an imaginary unit.

Calorimetric Measurements

The curing reaction of the different epoxy resins is investigated by means of a Netzsch differential scanning calorimeter DSC STA 449 F1 apparatus, under nitrogen flow, using an alumina crucible (Ahlden, Germany). The apparatus was calibrated utilizing indium and aluminum standards. To measure the residual heat of reaction, the samples were maintained at 30 °C for various durations (5 min, 10 min, 15 min, 30 min, 45 min, 60 min, up to 15 h) and then heated up to 250 °C at a rate of 10 °C min^{-1} (dynamic scan) at the end of each isotherm.

After curing, the glass-transition temperature was measured by applying the following temperature cycle: the sample was maintained at -30 °C for 2 min, followed by heating to a temperature of 150 °C at a rate of 20 °C min^{-1} .

Table I. Thinners Added to the Epoxy–Amine System

Thinners	Chemical structure
Methyl octanoate	
<i>o</i> -Xylene	
Butyl glycidyl ether	
Benzyl alcohol	
Epoxidized soybean oil	

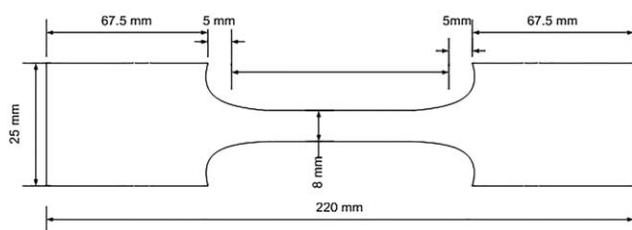


Figure 1. Tensile specimen.

Fourier Transform Infrared Spectroscopy

Fourier transform infrared spectroscopy with attenuated total reflection (ATR-FTIR) measurements were performed at ambient temperature using a Bruker Optik Spectrometer, Tensor 27 model, (Massachusetts, United States) with spectral range coverage from 4000 to 400 cm^{-1} . The spectra were measured at 4 cm^{-1} resolution over eight scans. The cured epoxy resin samples were ground and placed onto the crystal area. The sample thickness should be between 1 and 10 μm .

Dynamic Mechanical Analysis

Dynamic mechanical measurements were carried out with a DMA (dynamic mechanical analysis) Q800 (TA Instruments in Delaware, United States). The test consists of applying a tensile strain of 0.05% with a constant frequency of 1 Hz in a temperature sweep from -60 to 200 $^{\circ}\text{C}$ with a heating rate equal to 3 $^{\circ}\text{C}$ min^{-1} . The sample dimensions were 30 mm \times 10 mm \times 1 mm.

Tensile Properties

Tensile measurements were performed at three different cross-head speeds (1 mm min^{-1} , 10 mm min^{-1} , and 20 mm min^{-1}) with an Instron 5567 (Elancourt, France). Epoxy resin specimens were molded and cured at 30 $^{\circ}\text{C}$ and 48% relative humidity (RH) for 7 days. Specimen dimensions are represented in Figure 1. Each test was repeated at least three times.

RESULTS AND DISCUSSION

Rheological Measurements: Gel Point and Viscosity Measurements

The processing of thermosets is very much dependent on gelation and vitrification, two major structural transformations widely studied based on Gillam's adaptation of the time-temperature-transformation (TTT) cure diagram.³⁴

The gel time is a critical processing time because after the gel point the material is no longer able to flow and is therefore unprocessable. Various criteria are proposed in the literature for defining in a repeatable way, from rheological measurements, the gelation phenomenon:

- The point at which the viscosity suddenly diverges to infinity during steady shear flow measurements.
- The inflection point on the complex viscosity curve during oscillatory shear flow measurements.^{35,36}
- The point of inflection of the G' curve.³⁷
- The point of intersection of the G' and G'' curves: Tung and Dynes³⁸ proposed that the equality of G' and G'' may be used to define the gel point, while the work of Winter³⁹⁻⁴² has shown that this definition is not universal and only holds true for stoichiometrically balanced systems.

Thus, the crossover point of G' and G'' cannot be universally assigned as the gel point.

- The intersection of the $\tan(\delta)$ curves plotted as a function of time at different frequencies: at $t = t_{\text{gel}}$, $\tan(\delta)$ is independent of the stress frequency [$\tan(\delta)$ being defined by the ratio between G'' and G'].

The viscous properties are predominant in the liquid state, so $G'' > G'$ and $\tan(\delta) > 1$. As the time increases, the structure changes and G' and G'' rise. Moreover, the storage modulus grows more rapidly and crosses over the loss modulus when the gelation starts at a certain time corresponding to the gel point.⁴⁰ After this point, the elastic properties dominate and more energy is stored than dissipated, so $G'(\omega) > G''(\omega)$ and $\tan(\delta) < 1$. It is for this reason that the intersection of the curves of G' and G'' [$\tan(\delta) = 1$] was a criterion widely used for determining the gel time. However, additional studies have shown that the time needed to reach $\tan(\delta) = 1$ increases with the frequency of the rheological test. The gel point is considered as an intrinsic characteristic of the material.³⁹ Therefore, it is independent of the experimental conditions, and, as a consequence, it cannot correspond to the intersection of the G' and G'' curves. Then, another criterion was proposed: the intersection of the $\tan(\delta)$ curves plotted as a function of time at different frequencies.⁴³

Eloundou studied⁴⁴ two types of epoxy-amine systems [a flexible epoxy-amine system based on diglycidylether of 1,4-butanediol (DGEBD) and 4,9-dioxo-1,12-dodecanediamine and a rigid epoxy-amine system based on diglycidyl ether of bisphenol A (DGEBA) and 4,4'-methylenebis(3-chloro-2,6-diethylaniline)] by the rheological method near the gel point. These systems were stoichiometrically balanced. He demonstrated that the intersection of the $\tan(\delta)$ curves as a function of time at different frequencies is close to the value of $\tan(\delta) = 1$. Consequently, the criterion of the intersection of the G' and G'' curves may be a good approximation in some cases.

In the present work, it was considered that the addition of the different thinners with a low amount does not significantly change the stoichiometry of the epoxy-amine system. Hence, the gel point was estimated by the crossover of the storage $G'(\omega)$ and loss $G''(\omega)$ moduli curves monitored over time while conducting dynamic rheological measurements by the means of a plate-plate rheometer (Haake RheoWin RT 20).⁴⁰ Such curves are represented in Figure 2 for the epoxy-amine system without thinner. The criterion of the inflection point on the complex viscosity curve was also investigated. Figure 3 illustrates an example of viscosity curves recorded from the liquid state to after the gel point.

In order to identify the influence of the different thinners on the rheological properties of the epoxy-amine systems (gel point and viscosity), the thinners were added at the ratio of 5 wt % to the total mass of the resin.

Table II presents the resultant gel points of the different studied epoxy-amine systems obtained by the means of the two mentioned methods. It can be noted that the difference between the two methods is not significant: the maximum registered variance corresponds to 10%.

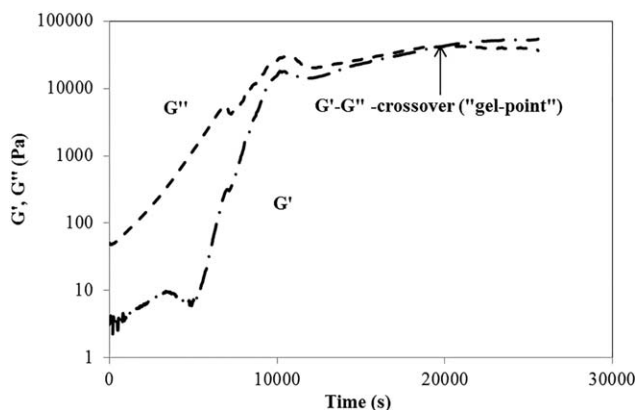


Figure 2. Evolution of viscous modulus G'' and elastic modulus G' over reaction time.

The obtained gel point of the epoxy resin without thinner is about 5 hours. Adding thinners decreased it significantly (Table II). Benzyl alcohol presents the lowest gel point (approximately 2

hours), which is too rapid to allow mortar processing to the final shape. Hence, benzyl alcohol was not considered further in this study.

The epoxy-amine system viscosity was measured during the cross-linking reaction by using the plate-plate rheometer. The obtained results (Figure 4) show that the introduction of the different thinners reduces the viscosity. The thinners in order of the viscosity they produced in the epoxy-amine system are as follows: butyl glycidyl ether < *o*-xylene < methyl octanoate < epoxidized soybean oil < benzyl alcohol. Admittedly, the *o*-xylene and the butyl glycidyl ether will improve the workability of resin mortars because they significantly decrease the viscosity of the polymeric binder. But, given that the implementation of these mortars is done in the open air and that these thinners are toxic and carcinogenic, their manufacture presents a danger to the operator and to the environment. It is desirable to use products with a minimum of risk. Methyl octanoate and epoxidized soybean oil are thinners of vegetal origin and are considered to be environmentally friendly products. Their low toxicity and nonflammability encouraged us to study their

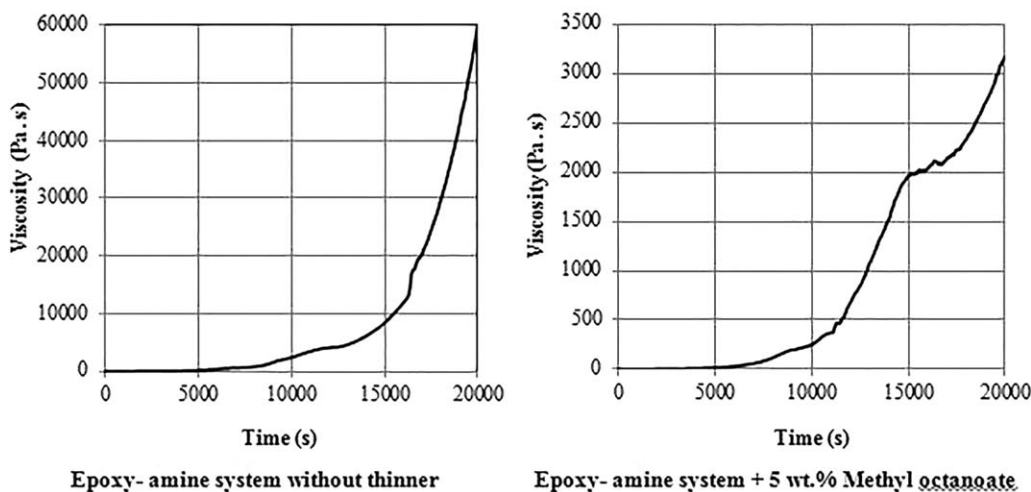


Figure 3. Viscosity curves recorded over reaction time from the liquid state to after the gel point.

Table II. Evolution of the Gel Point with the Nature of the Added Thinner at a Ratio of 5 wt % Obtained by the Crossover of the $G'-G''$ Curves and by the Inflection Point on the Viscosity Curve

Mixture	$G'-G''$ crossover	Inflection point on viscosity curve	Resulting difference between the two methods (%)
Epoxy-amine system without thinner	5 h	4 h 30 min	10
Epoxy-amine system + 5 wt % methyl octanoate	3 h 48 min	4 h	5
Epoxy-amine system + 5 wt % epoxidized soybean oil	3 h 40 min	3 h 34 min	2, 7
Epoxy-amine system + 5 wt % <i>o</i> -xylene	4 h 9 min	4 h 21 min	4, 6
Epoxy-amine system + 5 wt % butyl glycidyl ether	4 h 9 min	4 h 24 min	5, 7
Epoxy-amine system + 5 wt % benzyl alcohol	2 h 20 min	2 h 7 min	9, 3

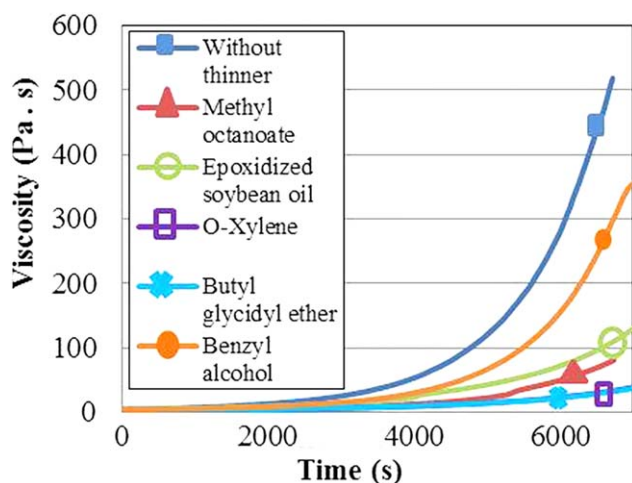


Figure 4. Evolution of the viscosity with the nature of the added thinner. [Color figure can be viewed in the online issue, which is available at wileyonlinelibrary.com.]

performances in improving resin mortar workability. However, we selected only methyl octanoate for economic reasons.

For an addition of 5 wt % of this thinner, the obtained gel points of the epoxy–amine system by the two methods (the crossover of the G' and G'' curves and the inflection point on the viscosity curve) differ only by 5%. Therefore, in the following, the gel point has been considered as the intersection of the G' and G'' curves for practical reasons.

In a second step, the effect of methyl octanoate at different rates of addition on the gel point of the epoxy–amine system was investigated. It was added at 2 wt %, 5 wt %, 7 wt %, and 9 wt % to the resin. It appears that, combined with the liquid epoxy resin, methyl octanoate reduces the gel time, which decreases from 5 hours to about 4 hours whatever the amount of the added thinner (Figure 5).

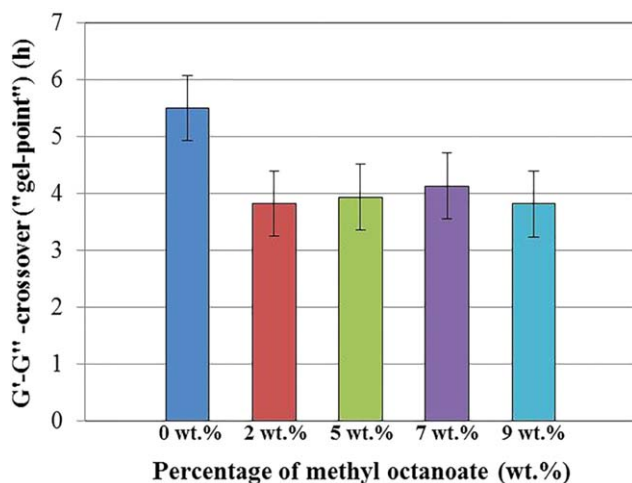


Figure 5. Evolution of $G'-G''$ crossover ("gel point") according to methyl octanoate amount. [Color figure can be viewed in the online issue, which is available at wileyonlinelibrary.com.]

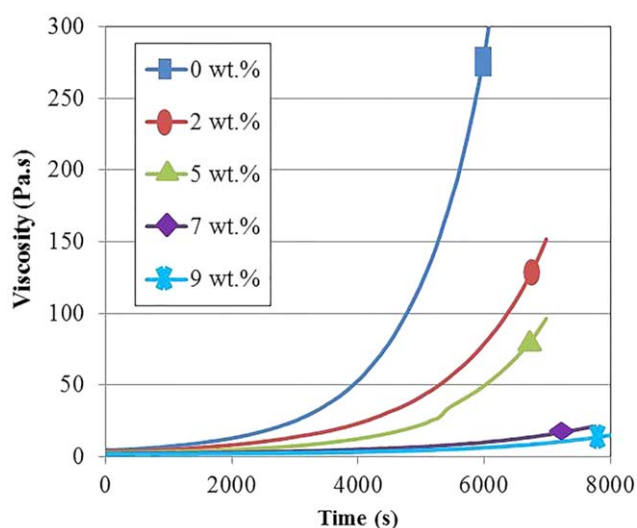


Figure 6. Evolution of viscosity over time according to the percentage of added methyl octanoate. [Color figure can be viewed in the online issue, which is available at wileyonlinelibrary.com.]

The viscosity of the epoxy–amine systems, mixed at 30 °C with different thinner concentrations, was measured as a function of time from the liquid state to after the gel point. The results (Figure 6) show that the introduction of methyl octanoate reduces significantly the viscosity of the mixture. The effect is proportional to concentration up to a concentration of 7 wt %, after which the viscosity is constant.

Infrared Spectroscopy Analysis of Raw Materials and Cured Epoxy Resins

Infrared Spectroscopy Analysis of Raw Materials: Prepolymer, Hardener, and Thinner. The infrared absorption spectra of prepolymer, hardener, and methyl octanoate (thinner) were recorded in the range 4000–400 cm^{-1} . The characteristic peaks, obtained through the analysis of the spectra (Table III, Table IV, and Table V) confirm that the products under study are respectively diglycidyl ether of bisphenol A (DGEBA), aliphatic amine hardener, and methyl octanoate.

In addition, the prepolymer infrared spectrum reveals other absorption bands located around 1455–1420, 862, and 712 cm^{-1} assigned to calcite, and others located around 1107, 1033, and 970 cm^{-1} corresponding to silica.

The infrared spectrum of the hardener indicates that the hardener contains benzyl alcohol and triethylenetetramine [1,2-ethanediamine- N,N' -bis(2-aminoethyl)-]. Triethylenetetramine is an aliphatic amine whose chemical formula is illustrated by Figure 7. Its presence is recognizable thanks to the N–H stretching (ν N–H), which is located between 3400 and 3300 cm^{-1} , the N–H deformation (δ N–H) situated at 1577 cm^{-1} , as well as the peaks at 1138 and 1081 cm^{-1} , which are respectively assigned to ν C–N (secondary amine) and ν C–N (primary amine).

The presence of benzyl alcohol in the hardener is discernible thanks to the O–H stretching (ν O–H) situated between 3400 and 3300 cm^{-1} (ν O–H is superimposed on ν N–H), the vibration modes of the aromatic ring, which are C=C group

Table III. Assignment of Principal Infrared Bands of Prepolymer

Wavenumber (cm ⁻¹)	Peak assignment	References
3501	ν O—H	45,47
3055	ν = C—H (aromatic)	
2924	ν (as) C—H	45,46
2870	ν (s) C—H	45,46
1607 / 1582 / 1508	ν C=C	45–48
1452	δ —C—H oxirane ring	45–48
1296	Group =C—O oxirane ring	45–48
916	Oxirane ring deformation	48
828	C—H phenyl	
1455–1420, 862, 712	Wave vibrations characteristic of calcite	49
1107, 1033, 970	Wave vibrations characteristic of silica	50

Table IV. Assignment of Principal Infrared Bands of Hardener

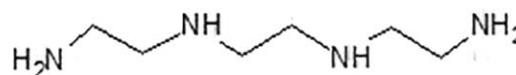
Wavenumber (cm ⁻¹)	Peak assignment	References
3400–3300	ν O—H and ? N—H	45–47
2919	ν (as) C—H	45, 46
2850	ν (s) C—H	45, 46
1577	δ N—H	45–48
≈1455	ν C=C (aromatic)	45,47
1138	ν C—N (secondary amine)	48
1081	ν C—N (primary amine)	48
823	δ C—H out of plane (aromatic)	47
698	δ C—H in the plane (aromatic)	47
1455–1420, 872, 712	Wave vibrations characteristic of calcite	48
1081, 1042, 1024, 698	Wave vibrations characteristic of silica	50

stretching, situated around 1455 cm⁻¹, as well as the off-plane and in-plane deformations occurring respectively around 823 cm⁻¹ and 698 cm⁻¹ (Table IV). Figure 8 represents the

Table V. Assignment of Principal Infrared Bands of Methyl Octanoate

Wavenumber (cm ⁻¹)	Peak assignment
2923	ν (as) C—H
2860	ν (s) C—H
1741	ν C=O (ester)
1437	δ C—H (CH)
1193	ν C—O (ester)
1164	ν C—O (ester)
730	δ C—H (CH ₂) out of plane

Assignments from Ref. 51.

**Figure 7.** Trientine.

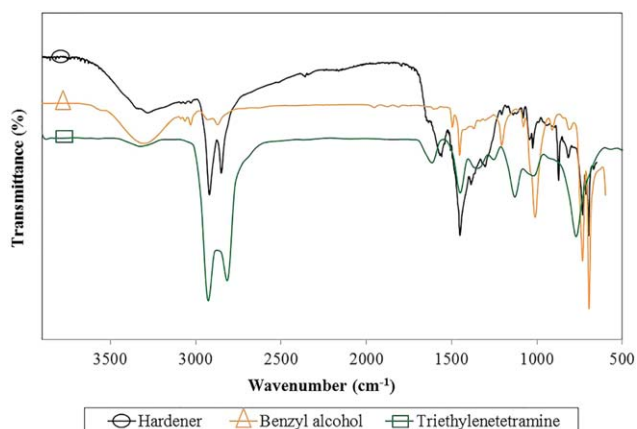
superimposed IR spectra of hardener, benzyl alcohol, and triethylenetetramine.

Calcite and silica fillers were identified in the hardener by means of the bands situated at 1455–1420, 872, and 712 cm⁻¹ attributed to calcite and 1081, 1042, 1024, and 698 cm⁻¹ attributed to silica fillers (Table IV).

Infrared Spectroscopy Analysis of the Different Cured Epoxy–Amine Systems. After mixing the thinner (methyl octanoate) with the prepolymer (DGEBA) and the hardener (aliphatic amine), the obtained system is cured at 30 °C and 48% RH until the end of curing. Different resin systems have been elaborated by varying the thinner amount. The chemical structure of the different epoxy–amine systems is studied through the FTIR technique in order to assess the reactivity of the thinner with the constituents of the resin.

To investigate the possibility of a reaction between methyl octanoate and the epoxy–amine system components, we chose to follow the evolution of the characteristic peak of methyl octanoate, which has the largest intensity, according to the percentage of addition. This peak is located at 1740 cm⁻¹ and is assigned to the carbonyl group (C=O). We also checked if there was an appearance of new IR peaks.

It can be observed (Figure 9) that the infrared spectra of the various epoxy–amine systems are identical except for the appearance of the peak situated at 1740 cm⁻¹ for the systems containing methyl octanoate. The intensity of this peak increases when the percentage of the thinner increases. This means that the methyl octanoate did not react with the components of the epoxy–amine system. According to the literature, the only possible reaction is amidification: it occurs between a fatty acid ester (methyl octanoate) and an amine (hardener). However, this reaction requires a high temperature (100 °C), which is not present for this

**Figure 8.** Superposed FTIR spectra of hardener, benzyl alcohol, and triethylenetetramine. [Color figure can be viewed in the online issue, which is available at wileyonlinelibrary.com.]

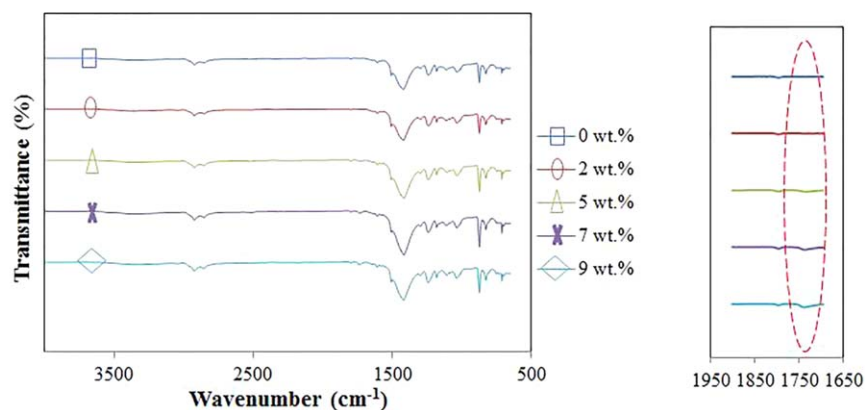


Figure 9. Superposed FTIR spectra of epoxy-amine systems cured with different amounts of methyl octanoate. [Color figure can be viewed in the online issue, which is available at wileyonlinelibrary.com.]

study.^{52,53} Hence, it can be confirmed that methyl octanoate did not react with the epoxy-amine system components.

Isothermal and Dynamic DSC Analysis of Epoxy-Amine System Curing Process

The reaction between the resin and the hardener is exothermic. The amount of heat is directly linked to the progress of the crosslinking reaction. One of the aims of this research is to quantify the effect of the thinner on the cure reaction. Hence the residual heat of reaction of each epoxy-amine system is measured after keeping it at 30 °C for various durations. Five epoxy-amine systems have been studied, differing by the amount of methyl octanoate (0 wt %, 2 wt %, 5 wt %, 7 wt %, and 9 wt %).

It can be noted that the exothermal peak area decreases as the duration of the curing increases (Figure 10).

Figure 11 reveals that the residual heat of reaction of all the epoxy-amine systems under study decreases as the duration of the isotherm increases. All the curves have the same shape. The crosslinking of all epoxy-amine systems tends toward its end

after approximately 18 hours. Hence, adding methyl octanoate, up to 9 wt %, to epoxy resin does not affect significantly the required duration to end crosslinking.

The measurement of the residual heat of reaction allows the degree of curing to be determined using the following eq. 5⁵⁴:

$$\alpha = \frac{\Delta H_t}{\Delta H_{\text{tot}}} = \frac{\Delta H_{\text{tot}} - \Delta H_{\text{res}}}{\Delta H_{\text{tot}}} \quad (5)$$

where ΔH_t represents the enthalpy of isothermal crosslinking at 30 °C after a duration t . The total enthalpy of crosslinking (ΔH_{tot}) was measured from the total area under the curve for a linear baseline obtained directly by a dynamic scan applied to the resin just after mixing.

The different studied systems show sigmoid-shaped curves (Figure 12), attesting that the cure reaction follows an autocatalytic mechanism.⁵⁵ The autocatalytic character is explained by the accumulation of hydroxyl groups formed during the curing. As the first reaction between the DGEBA and the amine hardener generates a hydroxyl group, there is an increase of the reaction rate at the beginning of crosslinking.

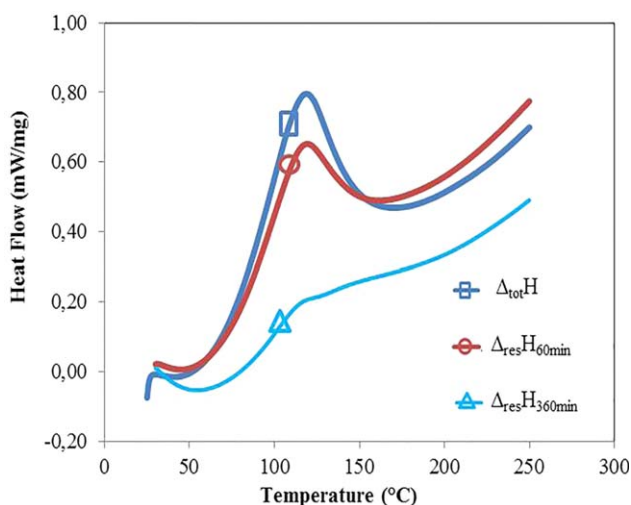


Figure 10. Residual heats of reaction of the mixture resin + hardener + 0 wt % methyl octanoate. [Color figure can be viewed in the online issue, which is available at wileyonlinelibrary.com.]

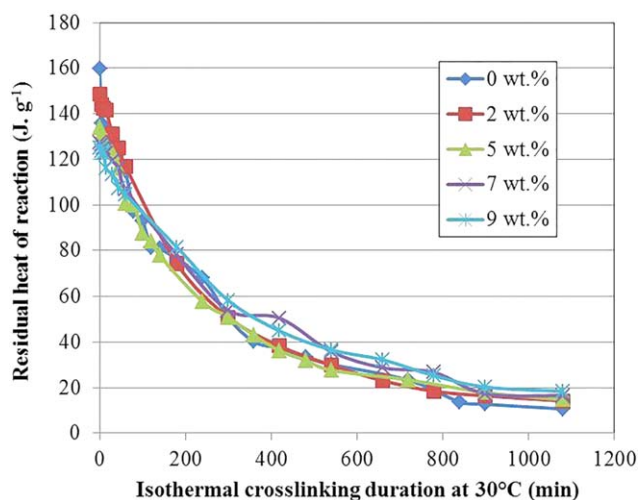


Figure 11. Evolution of the residual heat of reaction versus isothermal duration at 30 °C. [Color figure can be viewed in the online issue, which is available at wileyonlinelibrary.com.]

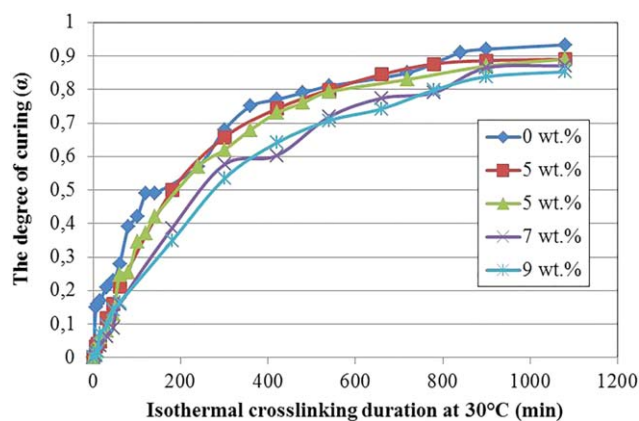


Figure 12. Evolution of the degree of curing versus isothermal duration at 30°C. [Color figure can be viewed in the online issue, which is available at wileyonlinelibrary.com.]

Figure 12 shows that the degree of curing of all the systems tends practically toward an asymptotic value of around 0.9 after 18 hours of curing at 30°C. It should be underlined that this value is slightly higher for the epoxy–amine system without thinner. Therefore, it can be assumed that the addition of methyl octanoate, up to 9 wt %, does not significantly affect the crosslinking duration of epoxy–amine resin or the corresponding degree of reticulation.

To investigate the effect of methyl octanoate on the kinetics of crosslinking, the reticulation reaction rate was calculated using eq. 6 and reported as a function of crosslinking duration (Figure 13).⁵⁴

$$\frac{d\alpha}{dt} = \frac{1}{\Delta H_{\text{tot}}} \times \frac{dH}{dt} \quad (6)$$

The maximum rate appears only a short time after the start of curing, which highlights the autocatalytic mechanism of the curing reaction. This characteristic remains unchanged even in the presence of methyl octanoate, but we have to notice from

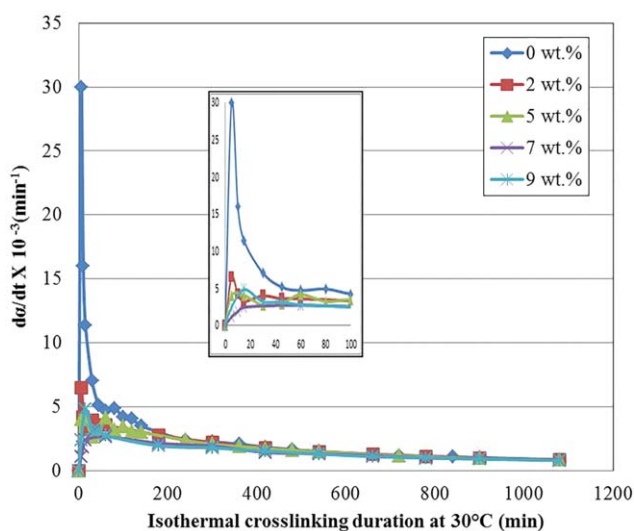


Figure 13. Reticulation reaction rate as a function of isothermal curing duration. [Color figure can be viewed in the online issue, which is available at wileyonlinelibrary.com.]

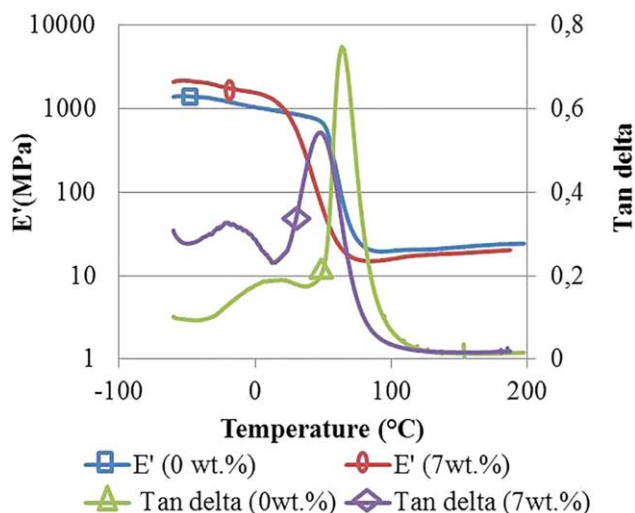


Figure 14. Evolution of the storage modulus (E') and $\tan \delta$ as a function of temperature of the epoxy–amine system and the epoxy–amine system cured with 7 wt % of methyl octanoate. [Color figure can be viewed in the online issue, which is available at wileyonlinelibrary.com.]

Figure 13 that introducing this thinner in the epoxy–amine system decreases the maximum rate of the curing reaction. As a result, this thinner slowed down the rate of reaction only at the beginning of curing.

Dynamic Mechanical Analysis

DMA tests were performed on the samples to investigate their mechanical properties in a temperature range of -60 to 200 °C.

Figure 14 illustrates the evolution of the storage modulus (E') and $\tan \delta$ as a function of temperature for the pure resin and for one containing 7 wt % of methyl octanoate. The $\tan \delta$ curve shows two types of relaxations: α relaxation (related to the rotation of main-chain polymer segments) and β relaxation (attributed to pendant group motions). It can be seen that the α relaxation peak, which is superposed on the glass-transition phenomenon, is shifted to lower temperatures when adding 7 wt % of thinner. Thus, there is a decrease of the glass-transition

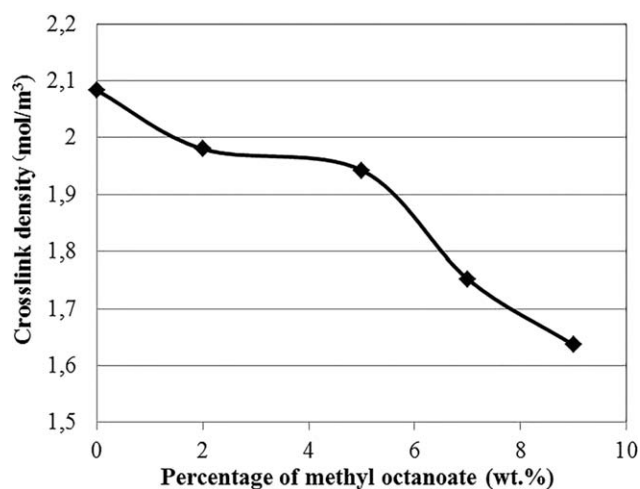


Figure 15. Evolution of crosslink density as a function of methyl octanoate percentage.

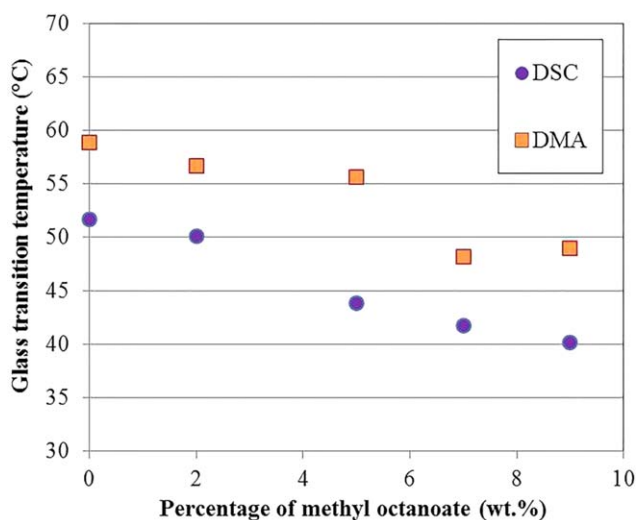


Figure 16. Evolution of glass-transition temperature as a function of the percentage of added methyl octanoate. [Color figure can be viewed in the online issue, which is available at wileyonlinelibrary.com.]

temperature. Furthermore, it should be noted that the $\tan \delta$ curve of the resin cured with an addition of 7 wt % of methyl octanoate presents a larger peak corresponding to β relaxation. At the macroscopic scale, these changes induce better toughness and ductile behavior during mechanical testing.^{32,56} DMA tests also allowed us to calculate the crosslink density of the different epoxy–amine systems in order to investigate the effect of methyl octanoate on this parameter. In fact, crosslink density is one of the most important factors determining the properties of cured thermoset resins.

Crosslink density was calculated through the measurements of the elastic modulus (E') of epoxy–amine systems in the rubbery plateau region; E' is directly related to this parameter according to the Flory relation [eq. 7]⁵⁷:

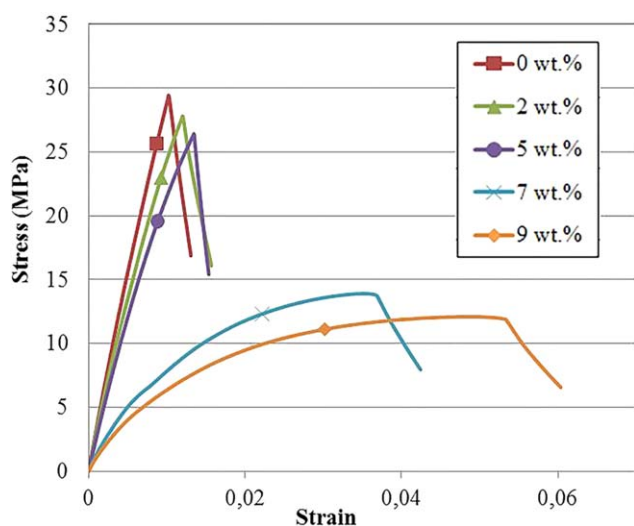


Figure 17. Evolution of stress–strain curves as a function of the percentage of added methyl octanoate at a tensile speed of 10 mm min⁻¹. [Color figure can be viewed in the online issue, which is available at wileyonlinelibrary.com.]

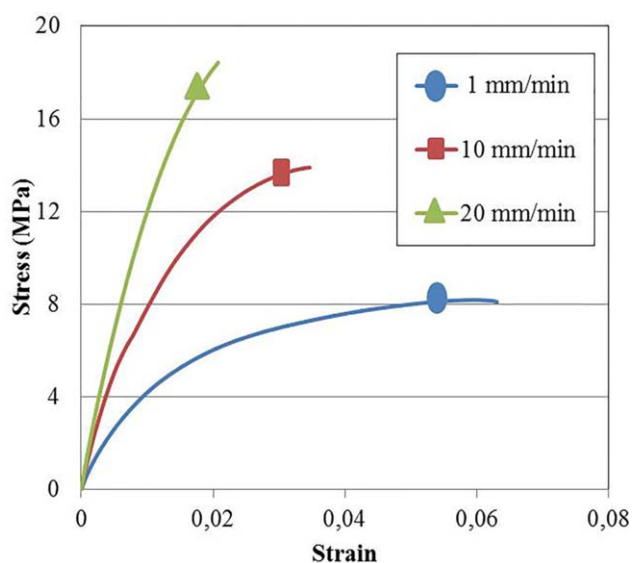


Figure 18. Evolution of stress–strain curves as a function of crosshead speed of resin cured with an addition of 7 wt % of methyl octanoate. [Color figure can be viewed in the online issue, which is available at wileyonlinelibrary.com.]

$$E' = 3 \cdot xRT \quad (7)$$

where E' is the elastic modulus in the rubbery plateau (Pa), x is the crosslink density of the epoxy resin (mol cm⁻³), R is the molar gas constant (8.314 J K⁻¹ mol⁻¹), and T is the temperature (K).

Figure 15 shows that increasing the methyl octanoate percentage leads to the decrease of the crosslink density. This evolution will have an impact on mechanical resistance.

Glass-Transition Measurements

The monitoring of structural modifications of materials can be obtained by determining the glass-transition temperature (T_g). Indeed, the T_g of the networks is related to their crosslinking density.⁵⁸ The T_g measurements were performed by DSC and DMA ($\tan \delta$ peak). The results are presented in Figure 16.

The glass-transition temperatures obtained by DMA are higher than those obtained by DSC. We notice that the addition of methyl octanoate causes a depression of the glass-transition temperature. The T_g values of cured epoxy gradually decreased with increasing thinner content. This evolution is explained by the decrease in crosslink density, as demonstrated by the DMA measurements.

Tensile Tests

Tensile testing was conducted to investigate the effect of methyl octanoate on epoxy resin tensile resistance. Tests were performed at three different crosshead speeds (1 mm min⁻¹, 10 mm min⁻¹, and 20 mm min⁻¹). The stress–strain curves (of unmodified and modified epoxy–amine systems) at a crosshead speed of 10 mm min⁻¹ are shown in Figure 17.

Clearly, the deformation at break of epoxy resin increases and the tensile strength decreases with the increase of methyl octanoate content. The strength is decreased by almost a factor of two when the concentration is higher than 5 wt %. This result was obtained for the different crosshead speeds.

The behavior becomes ductile by adding a quantity of methyl octanoate higher than or equal to 7 wt %. In fact, below this percentage, the behavior is brittle. Thus, an addition of 7 wt % marks a brittle–ductile transition. This result is attributed to the fact that the presence of methyl octanoate leads to the decrease in the crosslink density and then the decrease in mechanical strengths, which is in agreement with the results obtained by DMA (Figure 15).

Moreover, it can be noted (Figure 18) that increasing the crosshead speed induces an increase in tensile strength and a decrease in deformation at break of the cured epoxy–amine system. This behavior is observed for all studied compositions.

CONCLUSIONS

In this study, rheological measurements were carried out to identify the effect of different thinners on the gel point and the viscosity of an epoxy–amine system. The different thinners decreased the gelation time and showed viscosity-reducing ability. The optimum thinner (methyl octanoate) was evaluated to improve the workability of epoxy resin mortars and to be eco-friendly. Rheological measurements showed that its addition reduced the gel point of the epoxy–amine system independently of the added percentage. However, the viscosity of the mixture decreased as the rate of thinner increased up to the amount of 7 wt %. A thermal study (by isothermal and dynamic DSC) of the epoxy–amine system showed that the end of crosslinking is reached after approximately 18 hours of curing at 30 °C.

The measurement of the crosslinking rate revealed that the reaction follows an autocatalytic mechanism for all mixtures. Hence, the addition of methyl octanoate did not affect this characteristic; however, it slowed down the rate of reaction at the beginning of curing.

At a cured state, it was demonstrated by DMA and T_g measurements that the addition of methyl octanoate reduced the resin crosslink density.

It was also observed that the addition of this thinner affected the tensile resistance of the cured resin. The addition of 7 wt % of methyl octanoate marked a transition from a brittle elastic behavior to a ductile behavior.

ACKNOWLEDGMENTS

We are grateful for the funding obtained from Université de Tunis El Manar and Université de Cergy Pontoise to achieve this work. We also thank the financial support received from the CMCU PHC-Utique project (Campus France). Finally, we are grateful to Bostik for supplying the resin and for their help in carrying out this work.

REFERENCES

1. Park, S. J.; Bae, K. M.; Seo, M. K. *J. Ind. Eng. Chem.* **2010**, *16*, 337.
2. Frohlich, J.; Thomann, R.; Mulhaupt, R. *Macromolecules* **2003**, *36*, 7205.
3. Musto, P.; Ragosta, G.; Abbate, M.; Scarinzi, G. *Macromolecules* **2008**, *41*, 5729.
4. Sandler, J. K. W.; Kirk, J. E.; Kinloch, I. A.; Shaffer, M. S. P.; Windle, A. H. *Polymer* **2003**, *44*, 5893.
5. El-Tantawy, F.; Kamada, K.; Ohnabe, H. *Mater. Lett.* **2002**, *56*, 112.
6. Prasse, T.; Cavaille, J. Y.; Bauhofer, W. *Comp. Sci. Technol.* **2003**, *63*, 1835.
7. Martin, C. A.; Sandler, J. K. W.; Windle, A. H.; Schwarz, M. K.; Bauhofer, W.; Schultec, K.; Shaffer, M. S. P. *Polymer* **2005**, *46*, 877.
8. Soutis, C. *Prog. Aerosp. Sci.* **2005**, *41*, 143.
9. Soutis, C. *Mater. Sci. Eng. A* **2005**, *412*, 171.
10. Botelho, E. C.; Silvac, R. A.; Pardinia, L. C.; Rezende, M. C. *Mater. Res.* **2006**, *9*, 247.
11. Fowler, D. W. *Cement Concrete Comp.* **1999**, *21*, 449.
12. Gorninski, J.; Dal Molin, D.; Kazmierczak, C. *Cement Concrete Res.* **2004**, *34*, 2091.
13. Reis, J. M. L.; Ferreira, A. J. M. *Constr. Build. Mater.* **2004**, *18*, 523.
14. Gorninski, J. P.; Dal Molin, D. C.; Kazmierczak, C. S. *Constr. Build. Mater.* **2007**, *21*, 546.
15. Ohama, Y. *Adv. Cem. Based Mater.* **1997**, *5*, 310.
16. Chmielewska, B.; Czarnecki, L.; Sustersic, J.; Zajc, A. *Cement Concrete Comp.* **2006**, *28*, 803.
17. Ohama, Y. *Constr. Build. Mater.* **1996**, *10*, 77.
18. Ribeiro, M. C. S.; Reis, J. M. L.; Ferreira, A. J. M.; Marques, A. T. *Polym. Test.* **2003**, *22*, 849.
19. Golestaneh, M.; Amini, G. *World Appl. Sci. J.* **2010**, *9*, 216.
20. Haidar, M.; Ghorbel, E.; Toutanji, H. *Constr. Build. Mater.* **2011**, *25*, 1632.
21. Elalaoui, O.; Ghorbel, E.; Mignot, V.; Ben Oueddou, M. *Constr. Build. Mater.* **2012**, *27*, 415.
22. Jo, B. W.; Park, S. K.; Park, J. C. *Constr. Build. Mater.* **2008**, *22*, 2281.
23. Rebeiz, K. S.; Asce, M.; Craft, A. P. *J. Mater. Civil Eng.* **2004**, *16*, 15.
24. Rebeiz, K. S. *Cement Concrete Comp.* **1995**, *17*, 119.
25. Ribeiro, M. C. S.; Nóvoa, P. J. R. O.; Ferreira, A. J. M.; Marques, A. T. *Cement Comp.* **2004**, *26*, 803.
26. Ribeiro, M. C. S.; Reis, J. M. L.; Ferreira, A. J. M.; Marques, A. T. *Polym. Test.* **2003**, *22*, 849.
27. Vipulanandan, C.; Dharmarajan, N.; Ching, E. *Mater. Struct.* **1988**, *21*, 268.
28. El-Hawary, M.; Abdel-Fattah, H. *Constr. Build. Mater.* **2000**, *14*, 317.
29. Vipulanandan, C.; Dharmarajan, N. *Cement Concrete Res.* **1988**, *18*, 265.
30. In-Kwon, H.; Yong Soo, Y.; Seung-Bum, L. *J. Ind. Eng. Chem.* **2012**, *18*, 1997.
31. Medina Gonzalez, Y.; De Caro, P.; Thiebaud-Roux, S.; Lacaze-Dufaure, C. *J. Solution Chem.* **2007**, *36*, 437.
32. Czub, P. *Macromol. Symp.* **2006**, *245*, 533.

33. Mustata, F.; Tudorachi, N.; Rosu, D. *Compos. Part B*, **2011**, *42*, 1803.
34. Gillham, J. K. *Polym. Eng. Sci.* **1986**, *26*, 1429.
35. Ivankovic, M.; Incarnato, L.; Kenny, J. M.; Nicolais, L. *J. Appl. Polym. Sci.* **2003**, *90*, 3012.
36. Lelli, G.; Terenzi, A.; Kenny, J. M.; Torre, L. *Polym. Comp.* **2009**, *30*, 1–12.
37. Harran, D.; Laudouard, A. *Rheol. Acta* **1985**, *24*, 596.
38. Tung, C. Y. M.; Dynes, P. J. *J. Appl. Polym. Sci.* **1982**, *27*, 569.
39. Winter, H. H. *Polym. Eng. Sci.* **1987**, *27*, 1698.
40. Winter, H. H.; Chambon, F. *J. Rheol.* **1986**, *30* (2), 367.
41. Chambon, F.; Petrovic, Z. S.; MacKnight, W. J.; Winter, H. H. *Macromolecules* **1986**, *19*, 2146.
42. Chambon, F.; Winter, H. H. *J. Rheol.* **1987**, *31*, 683.
43. Pascault, J. P.; Sautereau, H.; Verdu, J.; Williams, R. J. J. In *Thermosetting Polymers*; Marcel Dekker Inc.: New York, **2002**; p 477.
44. Eloundou, J. P.; Ayina, O.; Ngamveng, J. N. *Eur. Polym. J.* **1998**, *34* (9), 1331.
45. Delor-Jestin, F.; Drouin, D.; Cheval, P. Y.; Lacoste, J. *Polym. Degrad. Stab.* **2006**, *91*, 1247.
46. Pei, Y. M.; Wang, K.; Zhan, M. S.; Xu, W.; Ding, X. J. *Polym. Degrad. Stab.* **2011**, *96*, 1179.
47. Musto, P.; Ragosta, G.; Russo, P.; Mascia, L. *Macromol. Chem. Phys.* **2011**, *202*, 3445.
48. Meure, S.; Wu, D. Y.; Furman, S. *Vib. Spectrosc.* **2010**, *52*, 10.
49. Dupuis, T.; Ducloux, J.; Butel, P.; Nahon, D. *Clay Miner.* **1984**, *19*, 605.
50. Saikia, J. B.; Parthasarathy, G. *J. Mod. Phys.* **2010**, *1*, 206.
51. Campbell, M. F.; Freeman, K. G.; Davidson, D. F.; Hanson, R. K. *J. Quant. Spectrosc. Radiat. Transfer* **2014**, *145*, 57.
52. Alam, M.; Alandis, N. J. *Polym. Environ.* **2011**, *19*, 391.
53. Rao, B. S.; Palanisamy, A. *Prog. Org. Coat.* **2008**, *63*, 416.
54. Thomas, R.; Durix, S.; Sinturel, C.; Omonov, T.; Goossens, S.; Groeninckx, G.; Moldenaers, P.; Thomas, S. *Polymer* **2007**, *48*, 1695.
55. Lee, J. Y.; Choib, H. K.; Shimc, M. J.; Kima, S. W. *Thermo-chim. Acta* **2000**, *343*, 111.
56. Czub, P.; Franek, I. *Polim.* **2013**, *58*, 135.
57. Cerrada, M. L.; De la Fuente, J. L.; Fernandez-Garcia, M.; Madruga, E. L. *Polymer* **2001**, *42*, 4657.
58. Di Marzio, E. A. *J. Res. Natl. Bur. Stand.* **1964**, *68A*, 611.